Infrared dielectric dispersion of $BaLiF_3$

1989 J. Phys.: Condens. Matter 1 5613

(http://iopscience.iop.org/0953-8984/1/33/004)

J. Phys.: Condens. Matter 1 (1989) 5613–5620. Printed in the UK

Infrared dielectric dispersion of $BaLiF_3$

A Boumriche†, P Simon‡, M Rousseau†, J Y Gesland† and F Gervais‡

† Laboratoire de Physique de l'Etat Condensé, UA 807 Université du Maine, 72017 Le Mans Cédex, France

‡ Centre de Recherche sur la Physique des Hautes Temperatures, CNRS, 45071 Orleans Cédex 2, France

Received 10 January 1989

Abstract. Infrared reflection spectra of the fluoperovskite $BaLiF_3$ have been measured in the range 20–4000 cm^{-1} at several temperatures. Frequencies, dampings and oscillator strengths of the three polar-phonon modes are reported. The polar-mode contribution to the dielectric constant has been calculated and compared with frequency dielectric measurements. All these results indicate that $BaLiF_3$ is one of the least anharmonic and most stable fluoperovskites.

1. Introduction

In recent years, many studies have been devoted to fluoperovskites AMF_3 (A = K, Rb, Cs, NH_4; M = Mg, Mn, Co, Ni, Zn, Cd, Ca). Most of these compounds crystallise in the cubic-perovskite type structure with one formula unit in the elementary cell, with space group O_h^1–Pm3m, and the atom in 0, 0, 0 (A), $\frac{1}{2}, \frac{1}{2}, \frac{1}{2}$ (M) and $\frac{1}{2}, \frac{1}{2}, 0$; $\frac{1}{2}, 0, \frac{1}{2}$; $0, \frac{1}{2}, \frac{1}{2}$ (F) positions. In some cases the cubic structure is not stable at room temperature under atmospheric pressure; the corresponding structures are then the so-called 'distorted perovskites'. These new phases are derived from the ideal structure by small atomic displacements such as MF_6 octahedra rotations. As previously mentioned by Rousseau *et al* (1975) and confirmed later by Boyer and Hardy (1981), the stability of different structures may be discovered through ionic-radius considerations. In the case of $BaLiF_3$, owing to the smallness of Li^+ ions, the stable arrangement of the ions is not the ideal perovskite one but an 'inverted perovskite structure' with the monovalent ion Li^+ at the centre of F_6 octahedron and the Ba^{++} divalent ion in the 12-fold environment site (figure 1). This original and unique situation among the AMF_3 family of compounds confers a particular interest to the study of the dynamical properties of $BaLiF_3$. In this paper we report infrared measurements at several temperatures in order to detect the eventual occurrence of a soft optical mode due to motion of the small Li^+ ions.

2. Experimental procedure

All measurements were performed on good-quality single crystals of $BaLiF_3$ grown by the Czochralski technique. The crystals were oriented, cut normal to the cubic axes and polished optically.

0953-8984/89/335613 + 08 $02.50

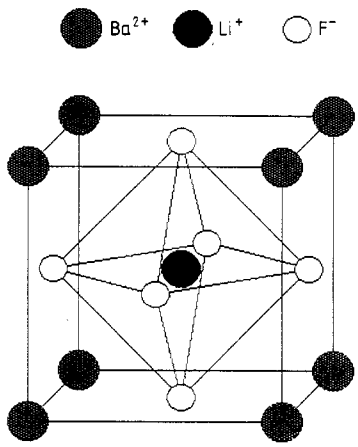

Figure 1. The 'inverted perovskite structure' $BaLiF_3$.

The infrared spectra were recorded with a Fourier-transform rapid-scan interferometer (Bruker IFS 113C) adapted for low- and high-temperature measurements (Gervais 1983). The experiments were performed at near-normal incidence (the incident light beam was at 6° from the normal of the crystal surface). Owing to the cubic symmetry, the three [100] axes are equivalent and the reflectivity measurements were carried out in the frequency range 20–1200 cm^{-1} with unpolarised light. Some spectra were recorded up to 4000 cm^{-1} in order to deduce the optical high-frequency dielectric constant ε_∞ from the reflectivity level.

The low-frequency dielectric constant was obtained using a Schering bridge (General Radio 716C) in the frequency range 100 Hz–100 kHz. For frequencies up to 30 MHz we used a '*Q*-metre' (Ferisol). The samples were rectangular slabs (thickness 1 mm, area 1 cm^2) with or without metallisation.

3. Results and discussion

Group-theory analysis shows that 15 lattice modes at $\boldsymbol{R} = \mathbf{0}$ transform under O_h^1 as $\Gamma = 4F_{1u} + F_{2u}$. Of these, there are $3F_{1u}$ infrared-active optical modes. The interaction of these polar modes with the coulombic electric field in the crystal gives rise to the TO–LO splitting corresponding to the reflection band widths observed in the infrared spectra (figure 2).

In order to determine the mode parameters accurately we have simulated the reflectance $R(\omega)$ via the Fresnel formula

$$R(\omega) = |[(\varepsilon(\omega))^{1/2} - 1]/[(\varepsilon(\omega))^{1/2} + 1]|^2 \tag{1}$$

with the dielectric function model shown in previous studies (Gervais 1983) to be convenient to represent even wide-band spectra

$$\varepsilon(\omega) = \varepsilon_\infty \prod_j (\Omega_{j\mathrm{LO}}^2 - \omega^2 + \mathrm{i}\gamma_{j\mathrm{LO}}\omega)/(\Omega_{j\mathrm{TO}}^2 - \omega^2 + \mathrm{i}\gamma_{j\mathrm{TO}}\omega). \tag{2}$$

With a fitting procedure it is possible to determine both the high-frequency permittivity ε_∞, the longitudinal $\Omega_{j\mathrm{LO}}$ and transversal $\Omega_{j\mathrm{TO}}$ optic mode frequencies and the

Table 1. Infrared-active mode frequencies, oscillator strengths, high-frequency and low-frequency dielectric constants of $BaLiF_3$ compared with equivalent values for $KZnF_3$ and $CsCaF_3$.

	Mode 1 (cm^{-1})		Mode 2 (cm^{-1})		Mode 3 (cm^{-1})						
	Ω_{TO}	Ω_{LO}	Ω_{TO}	Ω_{LO}	Ω_{TO}	Ω_{LO}	ε_∞	$\Delta\varepsilon_1$	$\Delta\varepsilon_2$	$\Delta\varepsilon_3$	$\varepsilon(0)$
$BaLiF_2$[a]	142	240	332	339	382	509	2.25	8.17	0.234	1.049	11.71
$BaLiF_3$[b]	151	232	376	377	450	567					
$KZnF_3$[c]	139	149	193	301	411	493	2.2	1.95	4.13	0.56	8.85
$KZnF_3$[d]	153	155	230	347	403	433					
$CsCaF_3$[c]	98	115	192	250	374	449	2.1	2.26	2.02	0.68	7.07
$CsCaF_3$[d]	89	102	233	294	410	448					

[a] Present results.
[b] Rigid ion model, Boumriche *et al* (1989).
[c] Ridou *et al* (1986).
[d] Rigid ion model, Rousseau *et al* (1981).

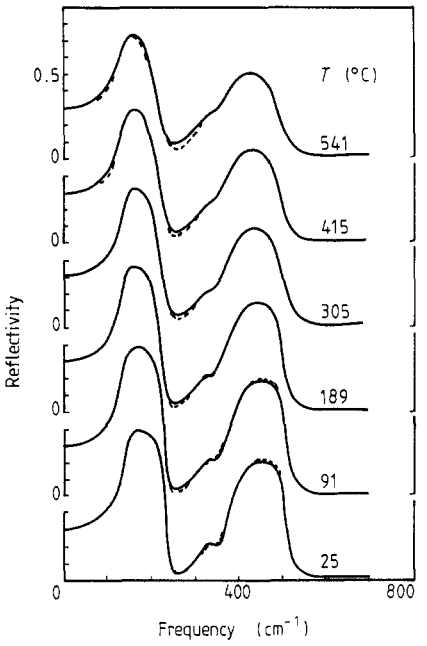

Figure 2. Temperature dependence of infrared reflectivity spectra of $BaLiF_3$. The full curves are the best fits with equation (3) of the experimental spectra (dashed curves).

corresponding dampings γ_{jLO} and γ_{jTO}. The frequencies are gathered in table 1 and compared with previous measurements by Ridou *et al* (1986) for cubic perovskites $KZnF_3$ and $CsCaF_3$. All these data are consistent with values obtained from lattice dynamical calculations with a rigid ion model (Rousseau *et al* 1981, Boumriche *et al* 1989). In this crystal, free from any phase transition, it is worth noticing that the frequencies obtained in this way are very close to these obtained with the Kramers–Kroning analysis. As shown in figure 2, the agreement between the measured and the calculated infrared spectra is very good in the considered temperature range 300–800 K. The temperature dependence of mode frequencies Ω_{jLO}, Ω_{jTO} is represented in figure 3.

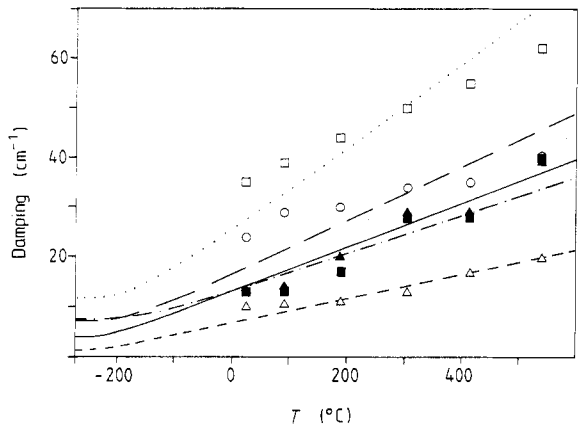

Figure 3. Temperature dependence of the TO-(open circles) and LO-(full circles) mode frequencies, obtained by simulation of spectra with the factorised form of the dielectric function.

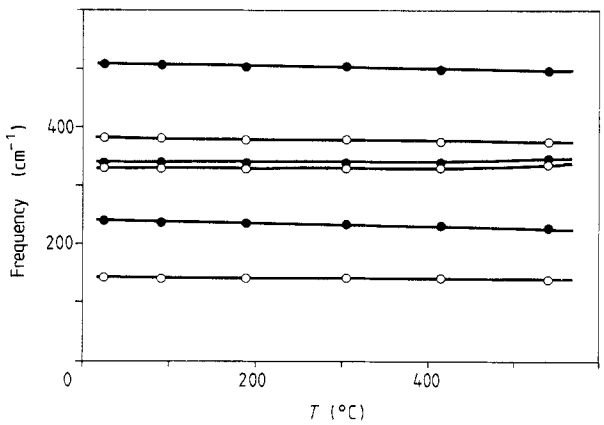

Figure 4. Temperature dependence of dampings. The symbols are the experimental values, and the curves are the best fits with equation (3): △ ----: mode TO1; ▲ ——: mode LO1; ○——: modes TO2 and LO2; □ · · · · ·: mode TO3; ■ —·—·: mode LO3 (the modes are numbered by order of increasing frequencies).

Table 2. Values of the adjustable parameter a_j defined in equation (3).

Mode	TO1	LO1	TO2–LO2	TO3	LO3
a_j	5	15.5	28	47	30

Figure 4 displays the temperature dependence of dampings. The following relation (Gervais 1983)

$$\gamma_j(T)_{\omega=\Omega_j} = \tfrac{1}{2}a_j[(\exp(\hbar\Omega_j/2kT) - 1)^{-1} + \tfrac{1}{2}] \tag{3}$$

where Ω_j is the frequency of mode j and a_j an adjustable parameter, has been proved in general cases to yield a correct description. It is based upon the assumption that lowest-order-additive anharmonic processes only are retained and that the phonons involved in such processes are distributed on both sides of the average frequency $\Omega_j/2$. The temperature dependences of anharmonic potentials and frequencies are also ignored. The best fits of equation (3) to experimental values are plotted in figure 4, and the corresponding values a_j are given in table 2. The agreement between experimental and calculated values is rather good for modes TO1, LO1 and LO3, and only fair for modes TO2–

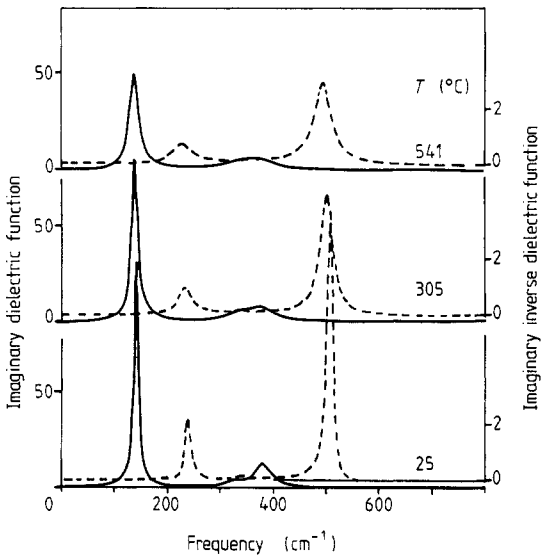

Figure 5. Temperature dependence of the structure of TO($\mathrm{Im}(\varepsilon)$) and LO ($\mathrm{Im}(1/\varepsilon)$) modes of $BaLiF_3$. Full curves: TO modes; dashed curves: LO modes.

LO2 and TO3. The structure of TO and LO modes deduced respectively from the imaginary part of the dielectric function and its inverse clearly shows (figure 5) the coupling of these modes. In this case, the damping behaviour involves some self-energy transfer between modes 2 and 3 and cannot be described by the simple model of equation (3).

The oscillator strength $\Delta\varepsilon_j$ of a polar vibration mode is fully defined when one considers the classical form of the dielectric function

$$\varepsilon(\omega) = \varepsilon_\infty + \sum_j \frac{\Delta\varepsilon_j \Omega_{j\mathrm{TO}}^2}{\Omega_{j\mathrm{TO}}^2 - \omega^2 + \mathrm{i}\gamma_{j\mathrm{TO}}\omega} \tag{4}$$

where each infrared-active normal mode is represented by a Lorentz resonant term with an additional phenomenological damping $\gamma_{j\mathrm{TO}}$. In the low frequency limit ($\omega \to 0$) the static dielectric constant $\varepsilon(0)$ is expressed as a sum over the electronic contribution ε_∞ and independent ionic contributions of each oscillator strength of the different infrared active modes

$$\varepsilon(0) = \varepsilon_\infty + \sum_j \Delta\varepsilon_j. \tag{5}$$

In practice, with the factorised form of the dielectric function the oscillator strength can be deduced from the TO–LO splitting of the normal modes through the relation

$$\Delta\varepsilon_j = \varepsilon_\infty((\Omega_{j\mathrm{LO}}^2/\Omega_{j\mathrm{TO}}^2) - 1) \prod_{k \neq j} (\Omega_{k\mathrm{LO}}^2 - \Omega_{j\mathrm{TO}}^2)/(\Omega_{k\mathrm{TO}}^2 - \Omega_{j\mathrm{TO}}^2). \tag{6}$$

The values obtained at several temperatures and the deduced static dielectric constants are reported in figure 6. As shown in figure 7, the room-temperature static dielectric constant calculated in this way is consistent with the near-constant value obtained by dielectric measurements in the frequency range 100 Hz–10 MHz. At higher frequency, for optical applications in the infrared region is it usual to define the dielectric properties with the real and imaginary parts of the indices of refraction. The frequency dependence of these two parameters is represented in figure 8.

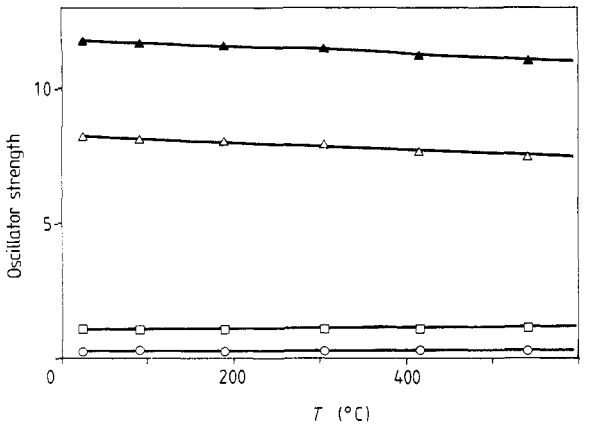

Figure 6. Temperature dependence of the oscillator strengths of TO modes. △: mode TO1; ○: mode TO2; □: mode TO3; ▲: dielectric constant calculated by equation (5).

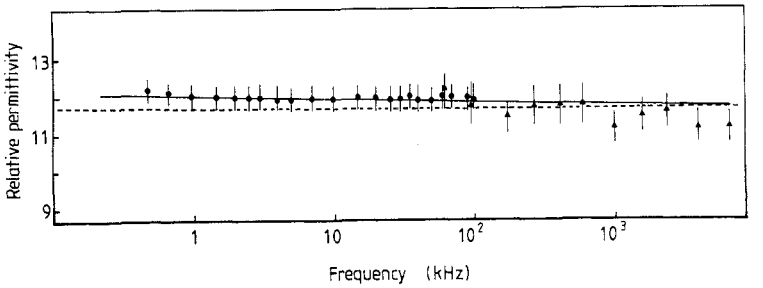

Figure 7. Frequency dependence of the dielectric permittivity in the low-frequency range. Black circles and triangles are obtained respectively with a Schering bridge, and a *Q*-metre. The dashed curve corresponds to the static dielectric constant deduced from infrared measurement.

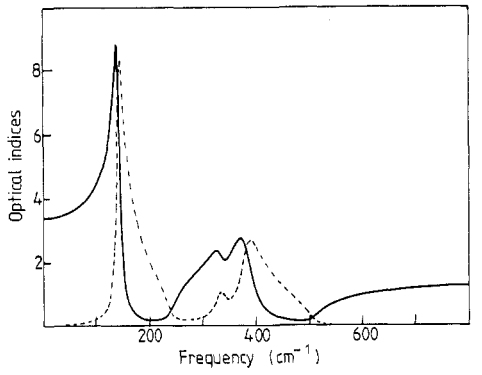

Figure 8. Frequency dependence of the indices of refraction (full curve) and of extinction (dashed curve), obtained by the fit of the factorised form of the dielectric function to experimental spectra at room temperature (25 °C).

As shown in table 1, the oscillator strength for mode 1 is much stronger in $BaLiF_3$ than in $KZnF_3$ and $CsCaF_3$. In fact the oscillator strength varies as the square of the dipole charge and the relative increment is very close to $(Z_{Ba}/Z_A)^2 = 4$. On the other hand, in $BaLiF_3$, as shown in figure 5, modes 2 and 3 are too close to be decoupled. In this case one may compare the sum $\Delta\varepsilon_2 + \Delta\varepsilon_3$ with the corresponding sum in $KZnF_3$

and $CsCaF_3$. As expected, these modes involving Li^+ motion in $BaLiF_3$ induce a smaller total oscillator strength than in $KZnF_3$ or $CsCaF_3$, where M^{++} divalent ions are involved.

From the TO–LO splitting of polar modes, as well as the oscillator strength, one may also calculate the ionic effective charge via the relation (Gervais and Arend 1983)

$$\sum_j (\Omega_{j\mathrm{LO}}^2 - \Omega_{j\mathrm{TO}}^2) = \frac{1}{\varepsilon_v V} \sum_k \frac{(Ze)_k^2}{M_k} \tag{7}$$

where e is the elementary electronic charge, Z_k the reduced effective ionic charge and ε_v the dielectric constant of the vacuum. The summation in the right-hand side is taken over all ions k with mass M_k located in the volume V of the unit cell, whereas the sum in the left-hand side is over all infrared-active-mode frequencies. The charge neutrality of the cell provides a second equation

$$Z_{\mathrm{Ba}} + Z_{\mathrm{Li}} + 3Z_{\mathrm{F}} = 0. \tag{8}$$

The remaining indeterminate (two equations but three unknowns) can be lifted in two successive steps, by decoupling the problem between modes external and internal to the octahedra. This is possible because there is only a small amount of dielectric dispersion (figure 5) between the lowest-frequency mode and both others. In the first step, one considers a system with rigid LiF_6 octahedra and then with only one polar mode, corresponding to motion of Ba against the (LiF_6) molecular group. This polar mode is the lowest-frequency TO mode in the experimental spectra, but its LO component ω_{LO}, in the absence of internal modes, does not coincide with the experimental lowest-frequency LO mode Ω_{LO}, the position of which is shifted by coupling with higher-frequency vibrations. Equation (7) then gives the effective charges carried by each of the two ions Ba and LiF_6. The left-hand side term, where the summation is limited to only the polar mode, is $(\omega_{\mathrm{LO}}^2 - \Omega_{\mathrm{TO}}^2)$, which, by using Lyddane–Sachs–Teller relation, can be rewritten as $(\Omega_{\mathrm{TO}}^2 \Delta\varepsilon/\varepsilon_\infty)$, where $\Delta\varepsilon$ is the oscillator strength of the polar mode. At room temperature, this gives $Z_{\mathrm{Ba}} = +2$, equal to the nominal charge. The effective charges cannot be evaluated with accuracy at higher temperatures because the volume thermal expansion is unknown.

With this value known from the first step, and now including all modes in the second step, equations (7) and (8) then give $Z_{\mathrm{Li}} = +0.6$ and $Z_{\mathrm{F}} = -0.87$. For comparison, the cationic effective charges evaluated by the same method in binary fluorides are $Z_{\mathrm{Ba}} = +1.8$ in BaF_2 (i.e., 90% of the nominal charge), and $Z_{\mathrm{Li}} = +0.72$ in LiF. Results in our ternary compound are thus found higher for Ba and lower for Li than in their binary compound with fluorine. This is one more example of a general behaviour, when comparing the cationic effective charges in binary and ternary compounds: of both cations in binary compounds, the most ionic has its ionic character further enhanced in the ternary compound, whereas of course the other cation is less ionic in the ternary than in the binary system.

4. Conclusion

In many stable fluoperovskites, AMF_3, some frequencies exhibit an upward shift with increasing temperature (Ridou *et al* 1986). This effect, similar to the behaviour expected for a soft ferroelectric mode in para-electric phase, is generally due to the large anharmonic motion of small M^{++} ions in large F_6 octahedra. The presence of small Li^+ ions in a structure naturally lead one to expect the occurrence of some effects associated with

large amplitudes of motion of these ions. In fact, when looking at the packing of the atoms in this inverted perovskite, it is clear that all ions contact each other and a near perfect close packing is achieved. This geometrical observation is consistent with both the absence of any soft optical mode and the weak frequency dependence of the static dielectric constant. Moreover, it is worth mentioning that no additional minor oscillator representing anharmonic multiphonon processes had to be added to enable the infrared reflectivity spectra to fit. For all these reasons, to the best of our knowledge, $BaLiF_3$ seems to be the least anharmonic and consequently the most stable compound of the AMF_3 fluoperovskites.

Acknowledgments

We are indebted to Dr A Bulou for help in the low-frequency dielectric constant measurements.

References

Boumriche A, Bulou A, Hennion B, Leblanc M and Rousseau M 1989 unpublished
Boyer L L and Hardy J R 1981 *Phys. Rev.* B **24** 2577
Gervais F and Arend H 1983 *Z. Phys.* B **50** 17
Gervais F 1983 *Infrared and Millimeter Waves* vol 8 ed. K J Button (New York: Academic) ch 7
Ridou C, Rousseau M and Gervais F 1986 *J. Phys. C: Solid State Phys.* **19** 5757
Rousseau M, Gesland J Y, Julliard J, Nouet J, Zarembowitch J and Zarembowitch J and Zarembowitch A 1975 *Phys. Rev.* B **12** 1579
Rousseau M, Gesland J Y, Hennion B, Heger G and Renker B 1981 *Solid State Commun.* **38** 45